We are IntechOpen,
the world's leading publisher of
Open Access books
Built by scientists, for scientists

4,800
Open access books available

122,000
International authors and editors

135M
Downloads

Our authors are among the

154
Countries delivered to

TOP 1%
most cited scientists

12.2%
Contributors from top 500 universities

BOOK CITATION INDEX
CLARIVATE ANALYTICS
INDEXED

WEB OF SCIENCE™

Selection of our books indexed in the Book Citation Index
in Web of Science™ Core Collection (BKCI)

Interested in publishing with us?
Contact book.department@intechopen.com

Numbers displayed above are based on latest data collected.
For more information visit www.intechopen.com

On the Thermal Transformer Performances

Ali Fellah and Ammar Ben Brahim
Gabes university, Engineers National School,
Applied Thermodynamic Research Unit, Gabes
Tunisia

1. Introduction

Different approaches are considered to select optimum criteria for technical process analysis. The maximization of the efficiency and the minimization of the total cost enclosing capital and running costs are the main purposes e.g. Munoz and Von Spakovsky (2003). Physical and thermodynamic criteria and technical and economic considerations have to be joined while analyzing energetic conversion processes (Berlitz et al. 1999; Chen 1995). Thus, deducing economic findings is the common objective of all intentions. Furthermore, the use of the interdisciplinary modeling methods has recently constituted the most important orientation of the technical system studies and process analyses. The simplification of both mathematical description and hypothesis definition of the interaction effects due to internal irreversibilities lead to the development of interesting simple but universal models. Internal irreversibilities due to heat transfer, throttling, mixing and internal dissipation of the working fluid, which are responsible for entropy generation are always present in a real heat driven refrigerator (Chen et Schouten, 1998). However, many works do not satisfy all the futures because the distribution of heat transfer properties between the components is taken as inputs and no as a result to be deduced from the optimization procedure.

In the other hand, the interaction effects in the internal processes do not favor separated studies. Therefore, it will be necessary to consider discreet parts of the whole system as they were independent. Then, the characteristics will be treated according to mathematical and physical couplings. To perform these approaches, the theory of finite time thermodynamic is mainly used. Seeing that the heat transfer processes are defined according to temperature finite difference method and the inner and outer reversibilities should be taken into consideration (Fellah et al., 2010). According to the study's finality, the decomposition of an overall system into subsystems may constitute a helpful tool, for which the physical and mathematical couplings would permit the efficient application of the investigation methods than a whole problem with a unique task. This could reduce the size of the mathematical problem. In fact, many attempts have been made to reduce the size of the problem, using the decomposition method on stage or/and on block models (Berlitz et al. 1999; Feidt and Lang 2002; Chen 1995; Chen and Wu 1996; Fellah, 2008 and Fellah et al., 2010).

The results obtained for various thermodynamic cycle analyses using FTT are closer to real device performance than those obtained using classical thermodynamics. During the last two decades, many optimization studies for refrigerators based on endoreversible and irreversible models have been performed by considering various objective functions. Wijeysundera, 1997;

Sahin et Kodal, 2003; Fellah et al. 2010, analyzed the performance of the three heat reservoir endoreversible cycle. Goktun, 1997 and Chen et Wu, 1996 analyzed the performance of three heat reservoir irreversible cycle. In both analyses Newton's heat transfer law is used.

From this context, Sokolov and Hersagal, (1993) optimized the system performance of a solar driven year-round ejector refrigeration system. Vargas et al. 1996 investigated the optimal condition for a refrigerator driven by a solar collector considering the three heat transfer irreversibility. Wijeysundera, 1997 and Bejan, (1995) analyzed a solar powered absorption cooling system using the three heat reservoir cycle including external heat transfer irreversibility. Later, Chen and Schouten, (1998) discussed the optimum performance of an irreversible absorption refrigeration cycle in which three external heat transfer irreversibilities have been considered.

Nevertheless, all those studies focus on the systems steady-state behavior. Vargas et al., (1998) and (2000) studied a transient endoreversible model of a heat driven refrigeration plant. The optimization is done from the point of view of the heat that drives the cycle. In their analyses, they concluded that the optimal fuel flow rate and minimum time to reach a prescribed cold space temperature are influenced by the thermal load in the refrigerated space and the thermal conductance of the walls. Recently, Vargas et al., (2000) optimized a solar collector driven water heating and absorption cooling plant using the three heat reservoir cycle.

Usually, real difficulties solving the optimization problem may appear owing to the significant number of unknowns. As a resolution to the above queries, an optimization of a thermodynamic cycle is carried out in the purpose to define the process optimal design parameters. As a case in point, the energetic process considered is a solar absorption refrigeration cycle. Two facets are considered for the investigation. Firstly, the methodology is based on the hierarchical decomposition, the endoreversibility principles and the Lagrange multipliers optimization method in a permanent regime. Secondly, the transient regime is considered.

2. Hypothesis

The analysis method, based on the endoreversible model, could be performed according to the following hypotheses which correspond to the nominal working conditions considered in the most process conceptual studies:

- The heat source temperatures are constant,
- The heat sources are reservoirs with fixed heat capacities,
- The overall heat transfer coefficients U_i of the heat exchangers and between the cycle and the surrounding reservoirs are constant,
- The system operates in a steady state,
- The heat transfer process between the work fluid and the source depends only on their temperatures.
- The heat transfers with the sources and the barriers are permanent and linear,
- The heat transfers between the subsystems and through the boundaries are the only sources of irreversibilities,
- All quantity entering in the system is considered as positive and all quantity coming out as negative,
- The heat exchangers operate in counter flow.

3. Hierarchical decomposition

There are three technical system decomposition types. The first is a physical decomposition (in equipment) used for macroscopic conceptual investigations. The second method is a disciplinary decomposition, in tasks and subtasks, used for microscopic analysis of mass and heat transfer processes occurring in different components. The third method is a mathematical decomposition associated to the resolution procedure of the mathematical model governing the system operating mode (Aoltola, 2003).

The solar absorption refrigeration cycle, presented on Fig. 1 (Fellah et al., 2010), is one of many interesting cycles for which great efforts have been consecrated. The cycle is composed by a solar concentrator, a thermal solar converter, an intermediate source, a cold source and four main elements: a generator, an absorber, a condenser and an evaporator. The thermal solar converter constitutes a first thermal motor TM_1 while the generator and the absorber constitute a second thermal motor TM_2 and the condenser and the evaporator form a thermal receptor TR. The exchanged fluxes and powers that reign in the different compartments of the machine are also mentioned. The parameterization of the cycle comprises fluxes and powers as well as temperatures reigning in the different compartments of the machine.

The refrigerant vapor, stemmed from the generator, is condensed and then expanded. The cooling load is extracted from the evaporator. The refrigerant vapor, stemmed from the evaporator, is absorbed by the week solution in the absorber. The rich solution is then decanted from the absorber into the generator through a pump.

The number of the decomposition levels must be in conformity with the physical bases of the installation operating mode. The mathematical identification of the subsystem depends on the establishment of a mathematical system with nil degree of freedom (DoF). Here, the decomposition consists in a four levels subdivision. The first level presents the compact global system which is a combination of the thermal motors TM_1 and TM_2 with the thermal receptor TR. After that, this level is decomposed in two sublevels the thermal converter TM_1 and the command and refrigeration system TM_2+TR. This last is subdivided itself to give the two sublevels composed by the thermal engine TM_2 and the thermal receptor TR. The fourth level is composed essentially by the separated four elements the generator, the absorber, the condenser and the evaporator. For more details see Fellah et al., 2010.

4. Optimization problem formulation

For heat engines, power-based analysis is usually used at maximum efficiency and working power, whereas the analysis of refrigerators is rather carried out for maximal cooling load. Therefore, there is no correspondence with the maximal value of the coefficient of performance COP. According to the objectives of the study, various concepts defined throughout the paper of Fellah et al. 2006 could be derived from the cooling load parameter e.g. the net Q_e, the inverse $1/Q_e$, the inverse specific A/Q_e cooling load.

For an endoreversible heat transformer (Tsirlin et Kasakov 2006), the optimization procedure under constraints can be expressed by:

$$\max_{u_i > 0} \left[P = \sum_{i=1}^{n} Q_i(T_i, u_i) \right] \qquad (1)$$
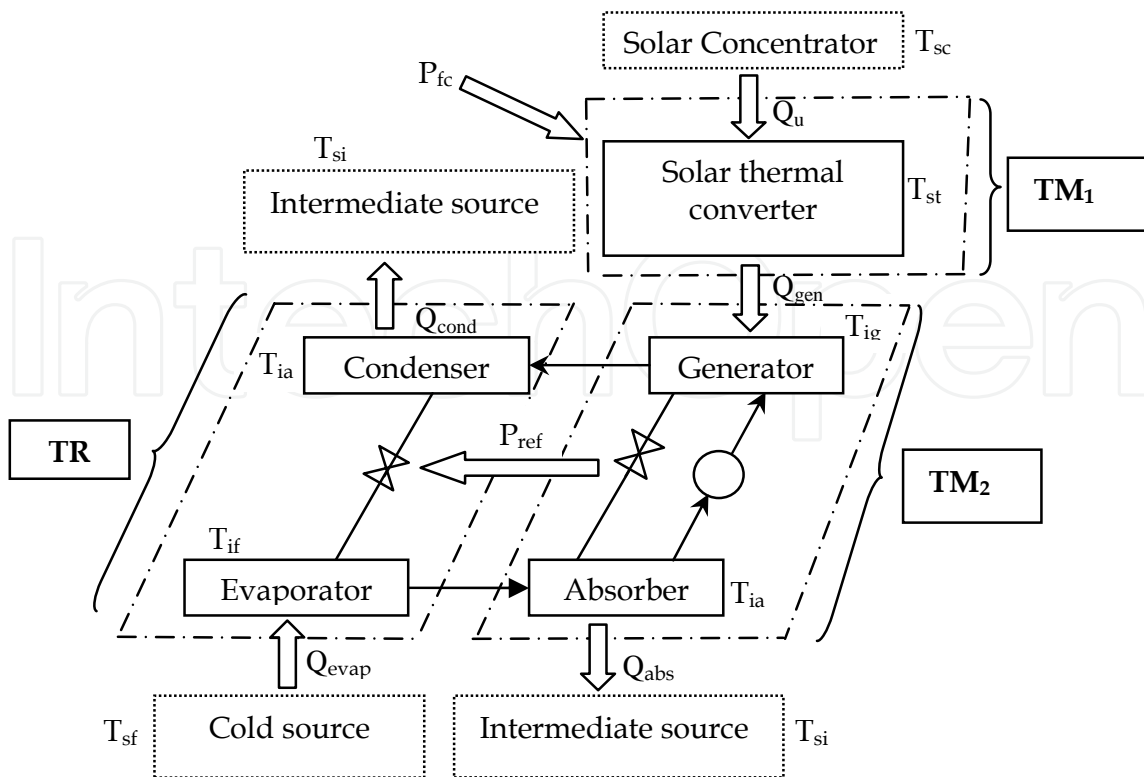
Fig. 1. Working principle and decomposition of a solar absorption refrigerator cycle

Under the constraints:

$$\sum_{i=1}^{n} \frac{Q_i(T_i, u_i)}{u_i} = 0 \tag{2}$$

And

$$\sum_{j=1}^{n} Q_{ij}(T_j, T_i) = Q_i(T_i, u_i) \quad i = 1,\ldots,m \tag{3}$$

where T_i : temperature of the ith subsystem

Q_{ij} : the heat flux between the ith and the jth subsystem

$Q(T_i, u_i)$: the heat flux between the ith subsystem and the transformer

P: the transformer power.

The optimization is carried out using the method of Lagrange multipliers where the thermodynamic laws constitute the optimization constraints. The endoreversible model takes into account just the external irreversibility of the cycle, consequently there is a minimization of the entropy production comparing to the entropy production when we consider internal and external irreversibilities.

For a no singular problem described by equations (1 to 3), the Lagrange function can be expressed as follows:

$$L = \sum_{i=1}^{m} Q_i + \sum_{i=m+1}^{n} Q_i - \Lambda \sum_{i=1}^{m} Q_i / u_i - \Lambda \sum_{i=m+1}^{n} Q_i / u_i + \sum_{i=1}^{m} \lambda_i \left(\sum_{j=1}^{n} Q_{ij} - Q_i \right) \tag{4}$$

Where λ_i and Λ are the Lagrange multipliers, m is the number of subsystems and n is the number of contacts.

According to the selected constraint conditions, the Lagrange multipliers λi are of two types. Some are equivalent to temperatures and other to dimensionless constants. The refrigerant temperatures in the condenser and the absorber are both equal to T_{ia}. Thus and with good approximation, the refrigeration endoreversible cycle is a three thermal sources cycle. The stability conditions of the function L for i> m are defined by the Euler-Lagrange equation as follows:

$$\frac{\partial L}{\partial u_i} = \frac{\partial}{\partial u_i}[Q_i(T_i, u_i)(1 - \Lambda/u_i)] = 0 \quad \text{Where } (i = m+1, \ldots, n) \tag{5}$$

5. Endoreversible behavior in permanent regime

5.1 Optimal characteristics

Analytical resolution delivers the following temperature distributions:

$$T_{ig}/T_{ia} = (T_{st}/T_{int})^{1/2} \tag{6}$$

$$T_{ie}/T_{ia} = (T_{cs}/T_{int})^{1/2} \tag{7}$$

$$T_{st}/T_{ia} = (T_{sc}/T_{int})^{1/2} \tag{8}$$

Expressions (6 to 8) relay internal and external temperatures. Generalized approaches (e.g. Tsirlin et Kasakov, 2006) and specific approaches (e.g. Tozer and Agnew, 1999) have derived the same distributions.

The thermal conductances UA_i, constitute the most important parameters for the heat transformer analysis. They permit to define appropriate couplings between functional and the conceptual characteristics. Considering the endoreversibility and the hierarchical decomposition principles, the thermal conductance ratios in the interfaces between the different subsystems and the solar converter, are expressed as follows:

$$UA_e / UA_{st} = I_{st}T_{ie}^{1/2}(T_{int}^{1/2} - T_{st}^{1/2}) / I_e T_{sc}^{1/2}(T_{ie}^{1/2} - T_{int}^{1/2}) \tag{9}$$

$$UA_g / UA_{st} = I_{st}T_{st}^{1/2} / I_g T_{sc}^{1/2} \tag{10}$$

$$UA_c / UA_{st} = I_{st}T_{int}^{1/2}(T_{int}^{1/2} - T_{st}^{1/2}) / I_a T_{sc}^{1/2}(T_{ie}^{1/2} - T_{int}^{1/2}) \tag{11}$$

$$UA_a/UA_{st} = I_{st}T_{int}^{1/2}/I_a T_{sc}^{1/2} \tag{12}$$

Where I_i represents the ith interface temperature pinch.

The point of merit is the fact that there is no need to define many input parameters while the results could set aside many functional and conceptual characteristics. The input parameters for the investigation of the solar refrigeration endoreversible cycle behaviors could be as presented by Fellah, 2008:

- The hot source temperature T_{sc} for which the transitional aspect is defined by Eufrat correlation (Bourges, 1992; Perrin de Brichambaut, 1963) as follows:

$$T_{sc} = -1.11t^2 + 31.34t + 1.90 \tag{13}$$

where t represents the day hour.
- The cold source temperature T_{sf}, 0°C ≤ T_{sf} ≤ 15°C
- The intermediate source temperature T_{si}, 25°C ≤ T_{si} ≤ 45°C.

For a solar driven refrigerator, the hot source temperature T_{sc} achieves a maximum at midday. Otherwise, the behavior of T_{sc} could be defined in different operating, climatic or seasonal conditions as presented in Boukhchana et al.,2011.

The optimal parameters derived from the simulation are particularly the heating and refrigerant fluid temperatures in different points of the cycle:
- The heating fluid temperature at the generator inlet T_{if},
- The ammonia vapor temperature at the generator outlet T_{ig},
- The rich solution and ammonia liquid temperatures at both the absorber and the condenser outlets T_{ia},
- The ammonia vapor temperature at the evaporator outlet T_{ie},

Relative stability is obtained for the variations of the indicated temperatures in terms of the coefficient of performance COP. However, a light increase of T_{ig} and T_{if} and a light decrease of Tia are observed. These variations affect slightly the increase of the COP. Other parameters behaviors could be easily derived and investigated. The cooling load Q_e increases with the thermal conductance increase reaching a maximum value and then it decreases with the increase of the COP. The decrease of Q_e is more promptly for great T_{sc} values. Furthermore, the increase of COP leads to a sensible decrease of the cooling load. It has been demonstrated that a COP value close to 1 could be achieved with a close to zero cooling load. Furthermore, there is no advantage to increase evermore the command hot source temperature

Since the absorption is slowly occurred, a long heat transfer time is required in the absorber. The fluid vaporization in the generator requires the minimal time of transfer. Approximately, the same time of transfer is required in the condenser and in the evaporator. The subsystem TM$_2$ requires a lower heat transfer time than the subsystem TR.

5.2 Power normalization

A normalization of the maximal power was presented by Fellah, 2008. Sahin and Kodal (1995) demonstrated that for a subsystem with three thermal reservoirs, the maximal power depends only on the interface thermal conductances. The maximal normalized power of the combined cycle is expressed as:

$$\tilde{P} = UA_2(UA_1 + UA_3)\big/\big[UA_2(UA_1 + UA_3) + UA_1\ UA_3\big] \tag{14}$$

Thus, different cases can be treated.

a. If $UA_1 \neq UA_2 \neq UA_3$ then $\tilde{P} < 1$. The power deduced from the optimization of a combined cycle is lower than the power obtained from the optimization of an associated endoreversible compact cycle.

b. If, for example $UA_1 = UA_3$; Then $\tilde{P}$ can be expressed as:

$$\tilde{P} = 1\big/\big[1 + 1/2\kappa^2\big] \tag{15}$$

where: $\kappa = \sqrt{UA_2/UA_1}$.

For important values of κ, equation (7) gives $\tilde{P} \approx 1$. The optimal power of the combined cycle is almost equal to the optimal power of the simple compact cycle.

c.   If $UA_1 = UA_2 = UA_3$ then $\tilde{P} = 2/3$. It is a particular case and it is frequently used as simplified hypothesis in theoretical analyses of systems and processes.

5.3 Academic and practical characteristics zones
5.3.1 Generalities
Many energetic system characteristics variations present more than one branch e.g. Summerer, 1996; Fellah et al.2006; Fellah, 2008 and Berrich, 2011. Usually, academic and theoretical branches positions are different from theses with practical and operational interest ones. Both branches define specific zones. The most significant parameters for the practical zones delimiting are the high COP values or the low entropy generation rate values. Consequently, researchers and constructors attempt to establish a compromise between conceptual and economic criteria and the entropy generation allowing an increase of performances. Such a tendency could allow all-purpose investigations.

The Figure 2 represents the COP variation versus the inverse specific cooling load (A_t/Q_{evap}) the curve is a building block related to the technical and economic analysis of absorption refrigerator. For the real ranges of the cycle operating variables, the curve starts at the point M defined by the smallest amount of (A/Q_e) and the medium amount of the COP. Then, the curve leaves toward the highest values in an asymptotic tendency. Consequently, the M point coordinates constitute a technical and economic criterion for endoreversible analyses in finite time of solar absorption refrigeration cycles Berlitz et al.(1999), Fellah 2010 and Berrich, 2011 . The medium values are presented in the reference Fellah, 2010 as follow:

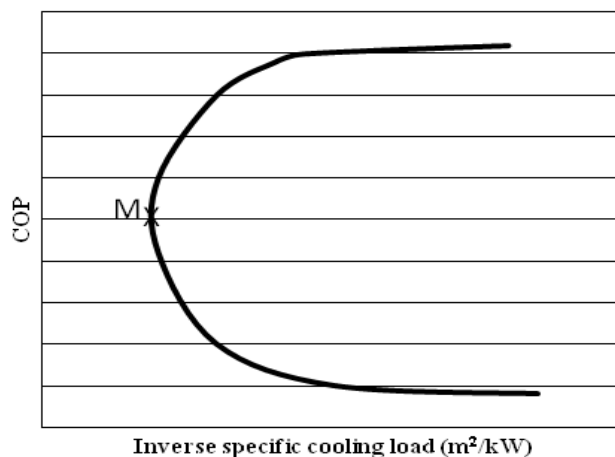$$0,4 \leq A / Q_e \leq 0,5 \, m^2 / kW \qquad (16)$$

Fig. 2. Inverse specific cooling load versus the COP.

5.3.2 Optimal zones characteristics
The Figure 3 illustrates the effect of the ISCL on the entropy rate for different temperatures of the heat source. Thus, for a Neat Cooling Load Q_e and a fixed working temperature T_{sc}, the total heat exchange area A and the entropy produced could be deduced.

The minimal entropy downiest zones are theses where the optimal operational zones have to be chosen. The point M is a work state example. It is characterized by a heat source

temperature of about 92°C and an entropy rate of 0.267kW/K and an A/Q_e equal to 24.9%. Here, the domain is decomposed into seven angular sectors. The point M is the origin of all the sectors.

The sector R is characterized by a decrease of the entropy while the heat source temperature increases. The result is logic and is expected since when the heat source temperature increases, the COP increases itself and eventually the performances of the machine become more interesting. In fact, this occurs when the irreversibility decreases. Many works have presented the result e.g. Fellah et al. 2006. However, this section is not a suitable one for constructors because the A/Q_e is not at its minimum value.
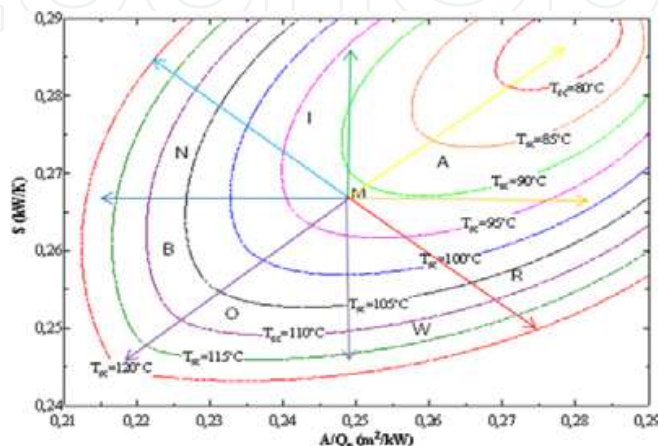
Fig. 3. Entropy rate versus the inverse specific cooling load.

The sector A is characterized by an increase of the entropy while the heat source temperature decreases from the initial state i.e. 92°C to less than 80°C. The result is in conformity with the interpretation highly developed for the sector R.

The sector I is characterized by an increase of the entropy rate while the heat source temperature increases. The reduction of the total area by more than 2.5% of the initial state is the point of merit of this sector. This could be consent for a constructor.

The sector N presents a critical case. It is characterized by a vertical temperature curves for low T_{sc} and a slightly inclined ones for high T_{sc}. Indeed, it is characterized by a fixed economic criterion for low source temperature and an entropy variation range limited to maximum of 2% and a slight increase of the A/Q_e values for high values of the heat source temperature with an entropy variation of about 6.9%.

The sector B is characterized by slightly inclined temperature curves for low T_{sc} and vertical ones for high T_{sc}, opposing to the previous zone. Indeed, the A/Q_e is maintained constant for a high temperature. The entropy variation attains a maximum value of 8.24%. For low values of the temperature, A/Q_e increases slightly. The entropy gets a variation of 1.7%. The entropy could be decreased by the increase of the heat source temperature. Thus it may be a suitable region of work.

As well, the sector O represents a suitable work zone.

The sector W is characterized by horizontal temperature curves for low T_{sc} and inclined ones for high T_{sc}. In fact, the entropy is maintained fixed for a low temperature. For high values of the temperature, the entropy decreases of about 8.16%. For a same heat source temperature, an increase of the entropy is achievable while A/Q_e increases. Thus, this is not the better work zone.

It should be noted that even if it is appropriate to work in a zone more than another, all the domains are generally good as they are in a good range:

$$0.21 < A/Q_e < 0.29 \ \text{m}^2/\text{kW} \tag{19}$$

A major design is based on optimal and economic finality which is generally related to the minimization of the machine's area or to the minimization of the irreversibility.

5.3.3 Heat exchange areas distribution

For the heat transfer area allocation, two contribution types are distinguished by Fellah, 2006. The first is associated to the elements of the subsystem TM_2 (command high temperature). The second is associated to the elements of the subsystem TR (refrigeration low temperature). For COP low values, the contribution of the subsystem TM_2 is higher than the subsystem TR one. For COP high values, the contribution of the subsystem TR is more significant. The contribution of the generator heat transfer area is more important followed respectively, by the evaporator, the absorber and the condenser.
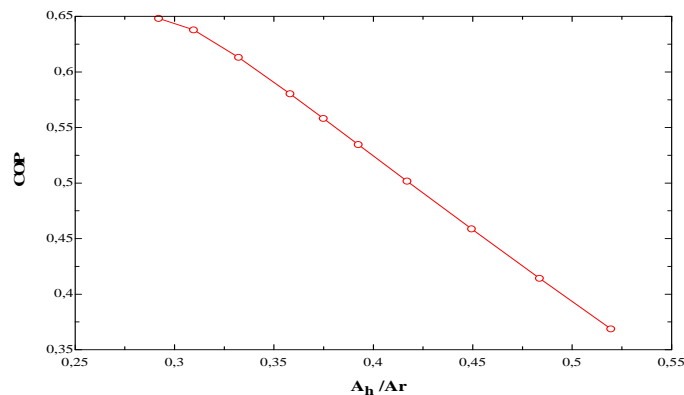
Fig. 4. Effect of the areas distribution on the COP

The increase of the ratio U_{MT2}/U_{RT} leads to opposite variations of the area contributions. The heat transfer area of MT_2 decreases while the heat transfer of TR increases. For a ratio U_{MT2}/U_{RT} of about 0.7 the two subsystems present equal area contributions.

The figure 4 illustrates the variation of the coefficient of performance versus the ratio A_h/A_r. For low values of the areas ratio the COP is relatively important. For a distribution of 50%, the COP decreases approximately to 35%.

6. Endoreversible behavior in transient regime

This section deals with the theoretical study in dynamic mode of the solar endoreversible cycle described above. The system consists of a refrigerated space, an absorption refrigerator and a solar collector. The classical thermodynamics and mass and heat transfer balances are used to develop the mathematical model. The numerical simulation is made for different operating and conceptual conditions.

6.1 Transient regime mathematical model

The primary components of an absorption refrigeration system are a generator, an absorber, a condenser and an evaporator, as shown schematically in Fig.5. The cycle is driven by the

heat transfer rate Q_H received from heat source (solar collector) at temperature T_H to the generator at temperature T_{HC}. Q_{Cond} and Q_{Abs} are respectively the heat rejects rates from the condenser and absorber at temperature T_{0C}, i.e.T_{0A}, to the ambient at temperature T_0 and Q_L is the heat input rate from the cooled space at temperature T_{LC} to the evaporator at temperature T_L. In this analysis, it is assumed that there is no heat loss between the solar collector and the generator and no work exchange occurs between the refrigerator and its environment. It is also assumed that the heat transfers between the working fluid in the heat exchangers and the external heat reservoirs are carried out under a finite temperature difference and obey the linear heat-transfer law ''Newton's heat transfer law''.
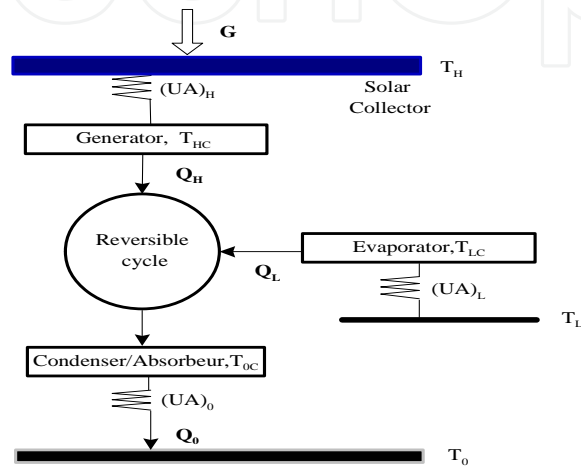
Fig. 5. The heat transfer endoreversible model of a solar driven absorption refrigeration system.

Therefore, the steady-state heat transfer equations for the three heat exchangers can be expressed as:

$$
\begin{aligned}
Q_L &= UA_L(T_L - T_{LC}) \\
Q_H &= UA_H(T_H - T_{HC}) \\
Q_0 &= UA_0(T_{0C} - T_0)
\end{aligned}
\tag{20}
$$

From the first law of thermodynamics:

$$
Q_H + Q_L = Q_0
\tag{21}
$$

According to the second law of thermodynamics and the endoreversible property of the cycle, one may write:

$$
\frac{Q_H}{T_{HC}} + \frac{Q_L}{T_{LC}} = \frac{Q_0}{T_{0C}}
\tag{22}
$$

The generator heat input Q_H can also be estimated by the following expression:

$$
Q_H = \eta_{sc} A_{sc} G_T
\tag{23}
$$

Where A_{sc} represents the collector area, G_T is the irradiance at the collector surface and η_{sc} stands for the collector efficiency. The efficiency of a flat plate collector can be calculated as presented by Sokolov and Hersagal, (1993):

$$Q_H = A_{st}G_Tb(T_{st} - T_H) \tag{24}$$

Where b is a constant and T_{st} is the collector stagnation temperature.

The transient regime of cooling is accounted for by writing the first law of thermodynamics, as follows:

$$mCv_{air}\frac{dT_L}{dt} = UA_w(T_0 - T_L) + Q_1 - Q_L \tag{25}$$

Where $UA_w (T_0-T_L)$ is the rate of heat gain from the walls of the refrigerated space and Q_1 is the load of heat generated inside the refrigerated space.

The factors UA_H, UA_L and UA_0 represent the unknown overall thermal conductances of the heat exchangers. The overall thermal conductance of the walls of the refrigerated space is given by UA_W. The following constraint is introduced at this stage as:

$$UA = UA_H + UA_L + UA_0 \tag{26}$$

According to the cycle model mentioned above, the rate of entropy generated by the cycle is described quantitatively by the second law as:

$$\frac{dS}{dt} = \frac{Q_0}{T_{0C}} - \frac{Q_H}{T_{HC}} - \frac{Q_L}{T_{LC}} \tag{27}$$

In order to present general results for the system configuration proposed in Fig. 5, dimensionless variables are needed. Therefore, it is convenient to search for an alternative formulation that eliminates the physical dimensions of the problem. The set of results of a dimensionless model represent the expected system response to numerous combinations of system parameters and operating conditions, without having to simulate each of them individually, as a dimensional model would require. The complete set of non dimensional equations is:

$$\begin{cases} \overline{Q}_L = z(\tau_L - \tau_{LC}) \\ \overline{Q}_H = y(\tau_H - \tau_{HC}) \\ \overline{Q}_0 = (1 - y - z)(\tau_{0C} - 1) \\ \overline{Q}_H = B(\tau_{st} - \tau_H) \\ \overline{Q}_H + \overline{Q}_L = \overline{Q}_0 \\ \dfrac{\overline{Q}_H}{\tau_{HC}} + \dfrac{\overline{Q}_L}{\tau_{LC}} = \dfrac{\overline{Q}_0}{\tau_{0C}} \\ \dfrac{d\tau_L}{d\theta} = w(\tau_0 - \tau_L) + \overline{Q}_1 - \overline{Q}_L \\ \dfrac{d\overline{S}}{d\theta} = \overline{Q}_0 - \dfrac{\overline{Q}_H}{\tau_H} - \dfrac{\overline{Q}_L}{\tau_L} \end{cases} \tag{28}$$

Where the following group of non-dimensional transformations is defined as:

$$\tau_H = \frac{T_H}{T_0} \quad , \quad \tau_L = \frac{T_L}{T_0} \quad , \tau_{st} = \frac{T_{st}}{T_0} \quad ,$$

$$\tau_{LC} = \frac{T_{LC}}{T_0} \quad , \tau_{OC} = \frac{T_{0C}}{T_0} \quad , \tau_{HC} = \frac{T_{HC}}{T_0} \quad ,$$

$$\overline{Q}_H = \frac{Q_H}{UA.T_0} , \overline{Q}_L = \frac{Q_L}{UA.T_0} , \overline{Q}_0 = \frac{Q_0}{UA.T_0} , \overline{Q}_1 = \frac{Q_1}{UA.T_0} ,$$

$$B = \frac{A_{sc} G_T b}{UA} , \theta = \frac{t.UA}{mCv_{air}}$$

(29)

B describes the size of the collector relative to the cumulative size of the heat exchangers, and y, z and w are the conductance allocation ratios, defined by:

$$y = \frac{UA_H}{UA} , z = \frac{UA_L}{UA} , w = \frac{UA_w}{UA}$$

(30)

According to the constraint property of thermal conductance UA in Eq. (26), the thermal conductance distribution ratio for the condenser can be written as:

$$x = \frac{UA_0}{UA} = 1 - y - z$$

(31)

The objective is to minimize the time θ_{set} to reach a specified refrigerated space temperature, $\tau_{L,set}$, in transient operation. An optimal absorption refrigerator thermal conductance allocation has been presented in previous studies e.g. Bejan, 1995 and Vargas et al., (2000) for achieving maximum refrigeration rate, i.e.,$(x,y,z)_{opt}$ =(0.5,0.25,0.25), which is also roughly insensitive to the external temperature levels (τ_H, τ_L). The total heat exchanger area is set to A=4 m^2 and an average global heat transfer coefficient to U=0.1 kW/m^{2}K in the heat exchangers and U_w=1.472 kW /m^{2}K across the walls which have a total surface area of A_w=54 m^2, T_0= 25°C and Q_1=0.8 kW. The refrigerated space temperature to be achieved was established at $T_{L,set}$=16°C.

6.2 Results

The search for system thermodynamic optimization opportunities started by monitoring the behavior of refrigeration space temperature τ_L in time, for four dimensionless collector size parameter B, while holding the other as constants, i.e., dimensionless collector temperature τ_H=1.3 and dimensionless collector stagnation temperature τ_{st}=1.6. Fig.6 shows that there is an intermediate value of the collector size parameter B, between 0.01 and 0.038, such that the temporal temperature gradient is maximum, minimizing the time to achieve prescribed set point temperature ($\tau_{L,set}$=0.97). Since there are three parameters that characterize the proposed system (τ_{st}, τ_H, B), three levels of optimization were carried out for maximum system performance.

The optimization with respect to the collector size B is pursued in Fig. 7 for time set point temperature, for three different values of the collector stagnation temperature τ_{st} and heat source temperatures τ_H=1.3. The time θ_{set} decrease gradually according to the collector size parameter B until reaching a minimum $\theta_{set,min}$ then it increases. The existence of an optimum with respect to the thermal energy input $\overline{Q}_H$ is not due to the endoreversible model aspects.

However, an optimal thermal energy input $\overline{Q}_H$ results when the endoreversible equations are constrained by the recognized total external conductance inventory, UA in Eq. (26), which is finite, and the generator operating temperature T_H.
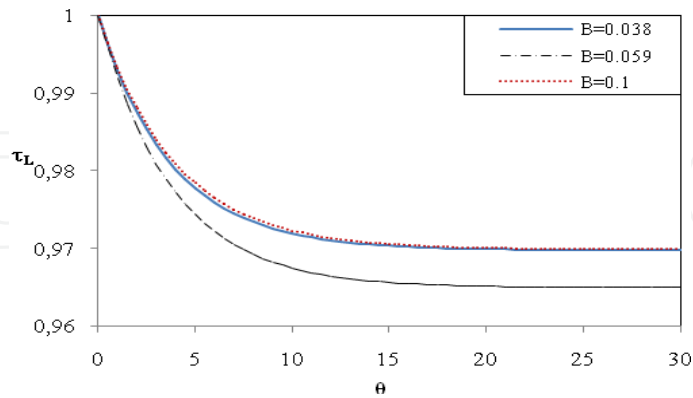

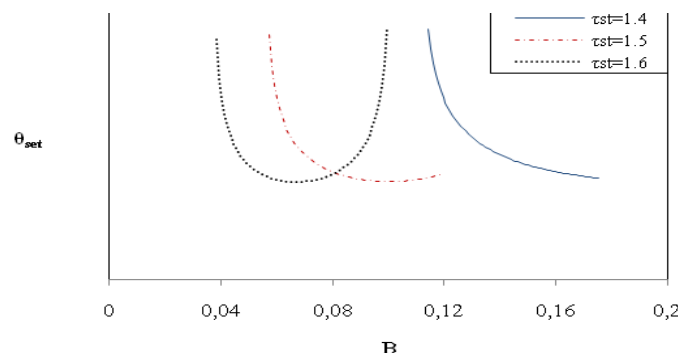Fig. 6. Low temperature versus heat transfer time for B=0.1,0.059,0.038.

Fig. 7. The effect of dimensionless collector size B on time set point temperature.

These constraints are the physical reasons for the existence of the optimum point. The minimum time to achieve prescribed temperature is the same for different values of stagnation temperature τ_{st}. The optimal dimensionless collector size B decreases monotonically as τ_{st} increases and the results are shown in Fig. 8. The parameter τ_{st} has a negligible effect on B_{opt} if τ_{st} is greater than 1.5 and B_{opt} is less than 0.1. Thus, τ_{sc} has more effect on the optimal collector size parameter B_{opt} than that on the relative minimum time.

The results plotted in Figures 8, 9 and 10 illustrate the minimum time $\theta_{set,min}$ and the optimal parameter B_{opt} respectively against dimensionless collector temperature τ_H, thermal load inside the cold space $\overline{Q}_1$ and conductance fraction w. The minimum time $\theta_{set,min}$ decrease and the optimal parameter B_{opt} increase as τ_H increase. The results obtained accentuate the importance to identify B_{opt} especially for lower values of τ_H. $\overline{Q}_1$ has an almost negligible effect on B_{opt}. B_{opt} remains constant, whereas an increase in $\overline{Q}_1$ leads to an increase in $\theta_{set,min}$. Obviously, a similar effect is observed concerning the behaviors of B_{opt} and $\theta_{set,min}$ according to conductance allocation ratios w.

During the transient operation and to reach the desired set point temperature, there is total entropy generated by the cycle. Figure 11 shows its behavior for three different collector size parameters, holding τ_H and τ_{st} constant, while Fig.12 displays the effect of the collector size
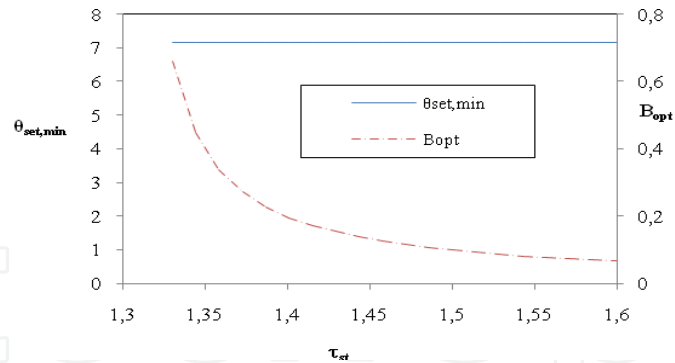
Fig. 8. The effect of the collector stagnation temperature τ_{st} on minimum time set point temperature and optimal collector size.
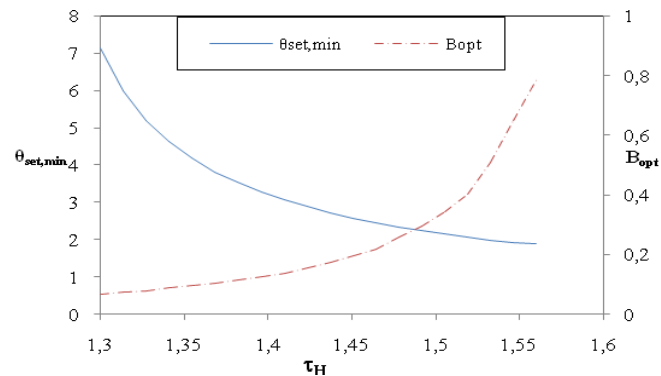

Fig. 9. The effect of dimensionless heat source temperatures τ_H on minimum time set point temperature and optimal collector size (τ_{st}=1.6).
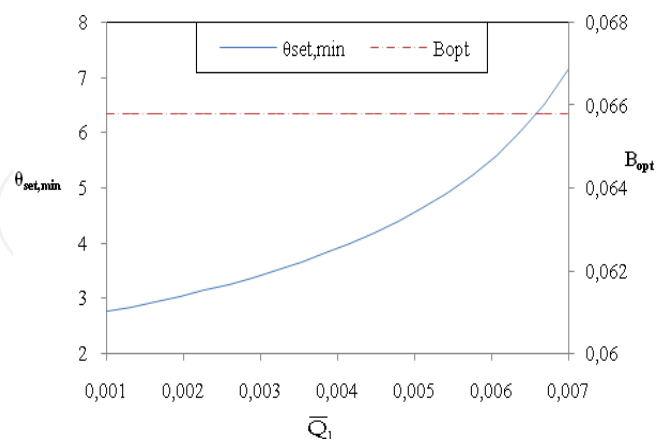

Fig. 10. The effect of thermal load in the refrigerated space on minimum time set point temperature and optimal collector size (τ_H=1.3 and τ_{st}=1.6).

on the total entropy up to θ_{set}. The total entropy increases with the increase of time and this is clear on the basis of the second law of thermodynamics, the entropy production is always positive for an externally irreversible cycle. There is minimum total entropy generated for a

certain collector size. Note that B_{opt}, identified for minimum time to reach $\tau_{L,set}$, does not coincide with B_{opt} where minimum total entropy occurs.
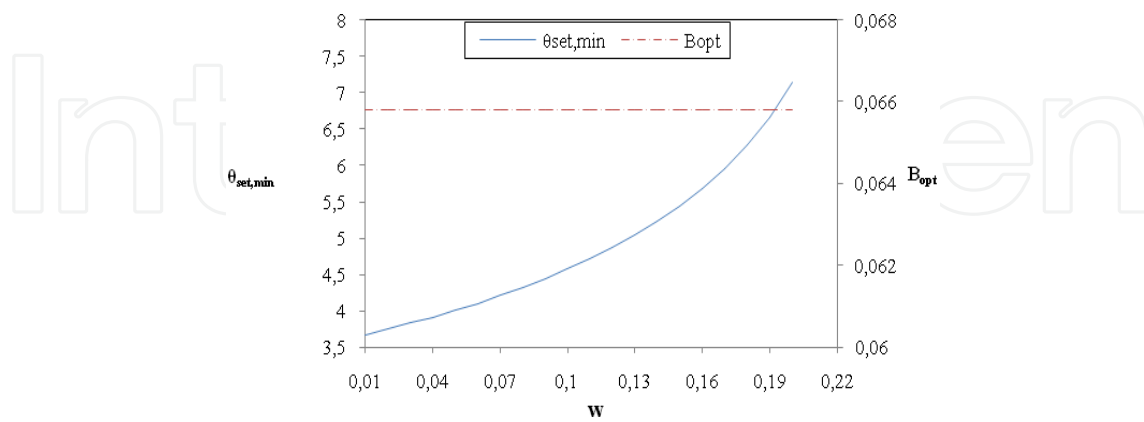
Fig. 11. The effect of conductance fraction on minimum time set point temperature and optimal collector size (τ_H=1.3 and τ_{st}=1.6).
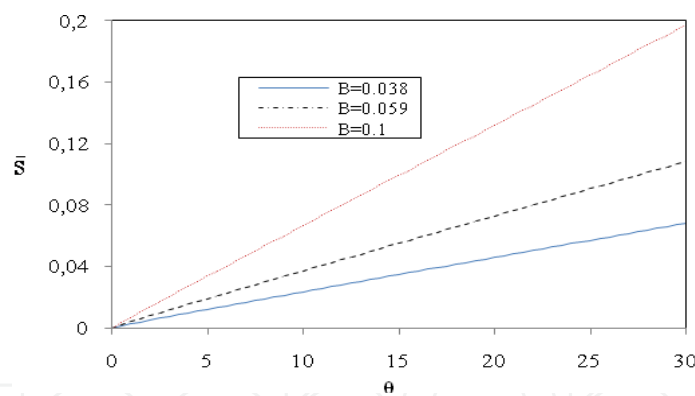
Fig. 12. Transient behavior of entropy generated during the time (τ_H=1.3 and τ_{st}=1.6).

Stagnation temperature and temperature collector effects on minimum total entropy generated up to θ_{set} and optimal dimensionless collector size are shown respectively in Figs.13 and 14. $\overline{S}_{set,min}$ is independent of τ_{st}, but, as the temperature stagnation increase B_{opt} decrease. This behavior is different from what was observed in the variation of temperature collector. An increase of stagnation temperature leads to a decrease of $\overline{S}_{set,min}$ and to an increase of B_{opt}. This result brings to light the need for delivering towards the greatest values of τ_{st} to approach the real refrigerator.

The optimization with respect to the size collector parameters for different values of τ_{st} is pursued in Figure 15 for evaporator heat transfer. There is an optimal size collector to attain maximum refrigeration.
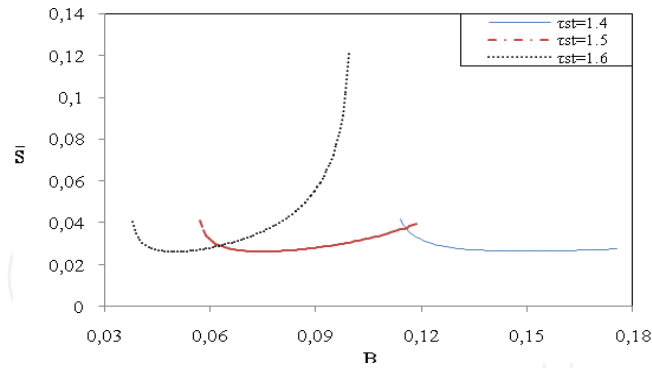
Fig. 13. Total entropy generated to reach a refrigerated space temperature set point temperature (τ_H=1.3)
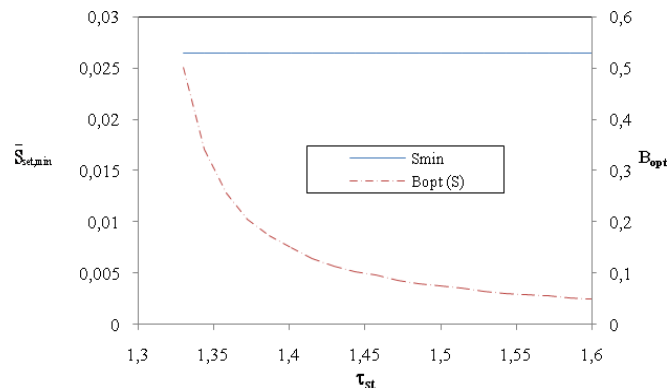

Fig. 14. The effect of dimensionless collector stagnation temperature, τst, on minimum entropy set point temperature and optimal collector size (τ_H=1.3).
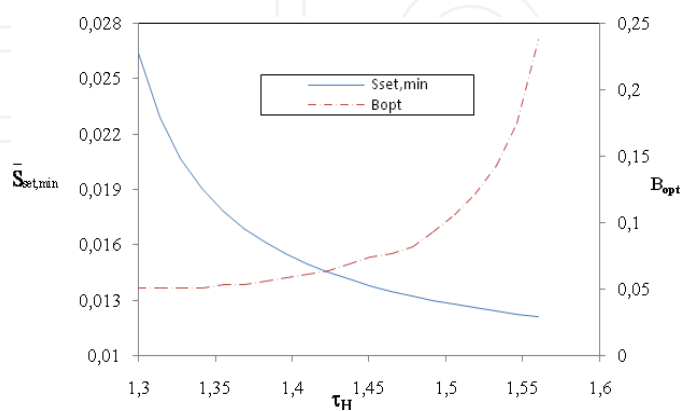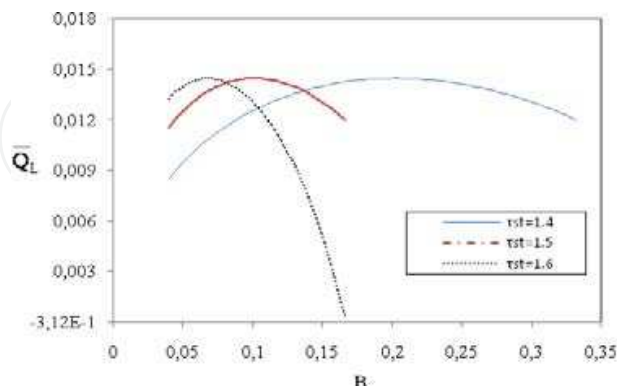

Fig. 15. The effect of dimensionless collector stagnation temperature, τ_H, on minimum entropy set point temperature and optimal collector size (τ_{st}=1.6).

Fig. 16. The effect of dimensionless collector size, B on heat exchanger Q_L (τ_H=1.3 and τ_L=0.97).

Finally, Figures 17 and 18 depict the maximization of the heat input to evaporator and optimal size collector with stagnation temperature and temperature collector, respectively. $\overline{Q}_{L,max}$ remains constant and B_{opt} decreases. On the other hand, the curves of Fig. 15 indicate that as τ_H increases, $\overline{Q}_{L,max}$ and B_{opt} increases. For a τ_H value under 1.35, B_{opt} is lower than 0.1.
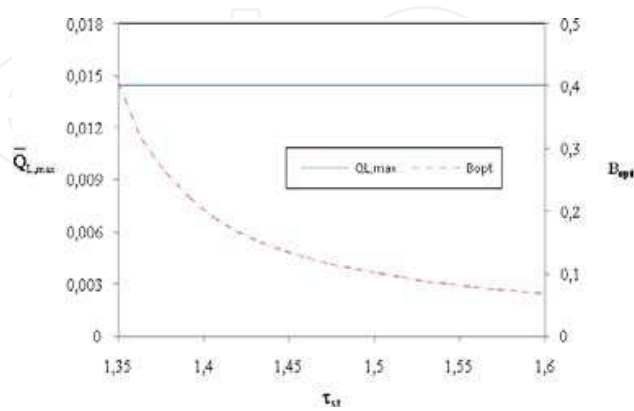
Fig. 17. Maximum heat exchanger, $Q_{L,max}$ to reached a refrigerated space temperature set point temperature (τ_H=1.3 and τ_L=0.97).
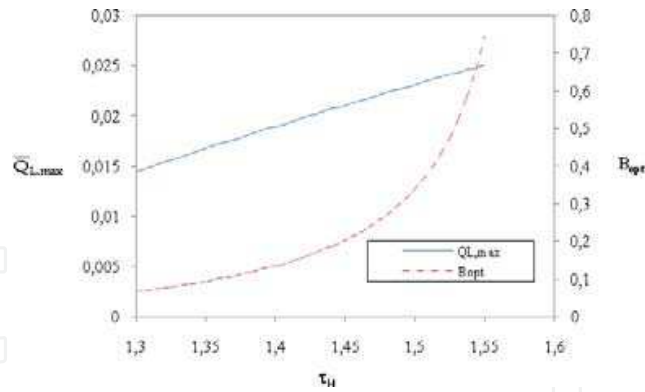
Fig. 18. Maximum heat exchanger, $Q_{L,max}$ to reached a refrigerated space temperature set point temperature (τ_{st}=1.3 and τ_L=0)

7. Conclusion

This chapter has presented an overview of the energy conversion systems optimization. Regarding the permanent regime, the functional decomposition and the optimization under constraints according to endoreversibility principles were the basis of the methodology. This procedure leads to a simple mathematical model and presents the advantage to avoid the use of equations with great number of unknowns. In so doing and as an example, the optimization of solar absorption refrigerator is investigated. The conceptual parameters are less sensible to temperature variations but more sensible to overall heat transfer coefficients variations. The couplings between the functional and conceptual parameters have permitted to define interesting technical and economical criteria related to the optimum cycle performances. The results confirm the usefulness of the hierarchical decomposition method in the process analyze and may be helpful for extended optimization investigations of other conversion energy cycles.

Also, the analysis in transient regime is presented. An endoreversible solar driven absorption refrigerator model has been analyzed numerically to find the optimal conditions. The existence of an optimal size collector for minimum time to reach a specified temperature in the refrigerated space, minimum entropy generation inside the cycle and maximum refrigeration rate is demonstrate. The model accounts for the irreversibilities of the three heat exchangers and the finiteness of the heat exchanger inventory (total thermal conductance).

8. References

Aoltola, J. (2003). Simultaneous synthesis of flexible heat exchanger networks. Thesis, Helsinky University of Technology

Bejan, A. (1995). Optimal allocation of a heat exchanger inventory in heat driven refrigerators", Heat Mass Transfer, vol.38, pp. 2997-3004,

Berrich, E.; Fellah, A.; Ben Brahim, A. & Feidt, M. (2011). Conceptual and functional study of a solar absorption refrigeration cycle. Int. J. Exergy vol.8,3, 265-280.

Boukhchana, Y.; Fellah, A.; & Ben Brahim, A. (2010). Modélisation de la phase génération d'un cycle de réfrigération par absorption solaire à fonctionnement intermittent. Int J Refrig. 34, 159-167

Bourges, B. (1992). Climatic data handbook for Europe. Kluwer,Dordrecht

Chen, J. (1995). The equivalent cycle system of an endoreversible absorption refrigerator and its general performance characteristics. Energy 20:995–1003

Chen, J. & Wu, C. (1996). General performance characteristics of an n stage endoreversible combined power cycle system at maximum specific power output. Energy Convers Manag 37:1401–1406

Chen, J. & Schouten, A. (1998). Optimum performance characteristics of an irreversible absorption refrigeration system", Energy Convers Mgmt, vol.39, pp. 999-1007,

Feidt, M. & Lang, S. (2002). Conception optimale de systèmes combinés à génération de puissance, chaleur et froid. Entropie 242:2–11

Fellah, A. ; Ben Brahim, A. ; Bourouis, M. & Coronas, A. (2006). Cooling loads analysis of an equivalent endoreversible model for a solar absorption refrigerator. Int J Energy 3:452–465

Fellah, A. (2008). Intégration de la décomposition hiérarchisée et de l'endoréversibilité dans l'étude d'un cycle de réfrigration par absorption solaire: modélisation et optimisation. Thesis, Université de Tunis-Elmanar, Ecole nationale d'ingénieurs, Tunis, Tunisia

Fellah, A.; Khir, T.; & Ben Brahim, A. (2010). Hierarchical decomposition and optimization of thermal transformer performances. Struct Multidisc Optim 42(3):437–448

Goktun, S. (1997). Optimal Performance of an Irreversible Refrigerator with Three Berlitz, J.T.; Satzeger, V.; Summerer, V.; Ziegler, F. & Alefeld, G. (1999). A contribution to the evaluation of the economic perspectives of absorption chillers. Int J Refrig 22:67–76

Martinez, P.J. & Pinazo, J.M. (2002). A method for design analysis of absorption machines. Int J Refrig 25:634–639

Munoz, J.R. & Von Spakovsky, M.R. (2003). Decomposition in energy system synthesis/design optimization for stationary and aerospace applications. J Aircr 40:35–42 Heat Sources", Energy, vol. 22, pp. 27-31,

Perrin de Brichambaut, Ch. (1963). Rayonnement solaire: échanges radiatifs naturels. Editions Gautier-Villars, Paris

Sahin, B. & Kodal, A. (1995). Steady state thermodynamic analysis of a combined Carnot cycle with internal irreversibility. Energy 20:1285–1289

Summerer, F. (1996). Evaluation of absorption cycles with respect to COP and economics, Int. J. Refrig., Vol. 19, No. 1, pp.19–24

Sokolov, M. & Hersagal, D. (1996). Optimal coupling and feasibility of a solar powered year-round ejector air conditioner", Solar Energy vol.50, pp. 507-516, 1993.

Tozer, R. & Agnew, B. (March 1999). Optimization of ideal absorption cycles with external irreversibilities. Int. Sorption Heat Pump Conference pp. 1-5, Munich,.

Tsirlin, A.M.; Kazakov, V.; Ahremenkov, A.A. & Alimova, N. A. (2006). Thermodynamic constraints on temperature distribution in a stationary system with heat engine or refrigerator. J.Phys.D: Applied Physics 39 4269-4277.

Vargas, J.V.C.; Horuz, I.; Callander, T. M. S.; Fleming, J. S. & Parise, J. A. R. (1998). Simulation of the transient response of heat driven refrigerators with continuous temperature control. Int. J. Refrig., vol.21, pp. 648–660,.

Vargas, J.V.C.;   Ordonez, J. C.; Dilay, A. & Parise. J. A. R. (2000). Modeling, simulation and optimization of a solar collector driven water heating and absorption cooling plant. Heat Transfer Engineering, vol.21, pp. 35-45,

Wijeysundera, N.E. (1997). Thermodynamic performance of solar powered ideal absorption cycles. Solar energy, pp.313-319
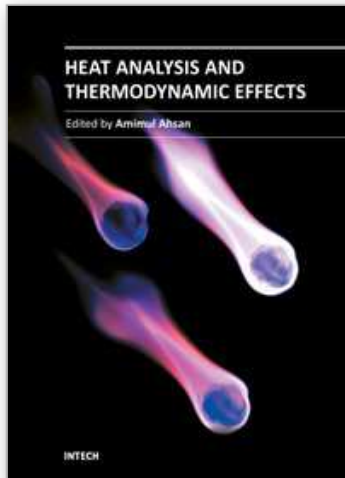
Heat Analysis and Thermodynamic Effects

Edited by Dr. Amimul Ahsan

The heat transfer and analysis on heat pipe and exchanger, and thermal stress are significant issues in a design of wide range of industrial processes and devices. This book includes 17 advanced and revised contributions, and it covers mainly (1) thermodynamic effects and thermal stress, (2) heat pipe and exchanger, (3) gas flow and oxidation, and (4) heat analysis. The first section introduces spontaneous heat flow, thermodynamic effect of groundwater, stress on vertical cylindrical vessel, transient temperature fields, principles of thermoelectric conversion, and transformer performances. The second section covers thermosyphon heat pipe, shell and tube heat exchangers, heat transfer in bundles of transversely-finned tubes, fired heaters for petroleum refineries, and heat exchangers of irreversible power cycles. The third section includes gas flow over a cylinder, gas-solid flow applications, oxidation exposure, effects of buoyancy, and application of energy and thermal performance index on energy efficiency. The forth section presents integral transform and green function methods, micro capillary pumped loop, influence of polyisobutylene additions, synthesis of novel materials, and materials for electromagnetic launchers. The advanced ideas and information described here will be fruitful for the readers to find a sustainable solution in an industrialized society.

How to reference

In order to correctly reference this scholarly work, feel free to copy and paste the following:

Ali Fellah and Ammar Ben Brahim (2011). On the Thermal Transformer Performances, Heat Analysis and Thermodynamic Effects, Dr. Amimul Ahsan (Ed.), ISBN: 978-953-307-585-3, InTech, Available from: http://www.intechopen.com/books/heat-analysis-and-thermodynamic-effects/on-the-thermal-transformer-performances

INTECH
open science | open minds